

## CHAPTER 85

### VISIBLE-REGION PHOTOGRAPHIC REMOTE SENSING OF NEARSHORE WATERS

Tsuguo Sunamura *Institute of Geoscience, University of Tsukuba,  
Ibaraki 300-31, Japan*  
Kiyoshi Horikawa *Department of Civil Engineering, University of  
Tokyo, Tokyo 113, Japan*

#### ABSTRACT

By use of a synchronized camera system, multiband black-and-white photographs and conventional color photographs were taken respectively with the purposes of testing filters available for shallow-water photographic bathymetry, and of checking the availability of low-cost process imagery for the study of coastal processes. Kodak Wratten filters 29, 58, and 90 were employed for the multiband photography. A Wratten 90 filter provided the best correlation between water depth and the photographic density. The low-cost imagery, obtained in a laboratory from the color photographs by applying ordinary filters without using any expensive image processing devices, proved to be useful.

#### INTRODUCTION

Since minimum attenuation of light in water occurs in the visible region of electromagnetic spectrum, i.e., 400-700 nm in wavelength, the remote sensors available in this region are effective for the aerial investigation of nearshore waters, especially of underwater environments. The photographic sensors covering the visible region are (1) black-and-white photographs, (2) color photographs, and (3) multiband or multispectral photographs; these sensors have been widely used in the field of coastal engineering ( Stafford, 1972 ).

The feasibility of nearshore bathymetry using multiband photographs has recently investigated ( Stafford, 1972 ), and several studies have been conducted to explore optimum film/filter combinations for the bathymetric use ( e.g., Lockwood et al., 1974; Magoon and Pirie, 1972; Pestrong, 1969 ). However, sufficient data on this point are unavailable. One of two purposes of the present study is to furnish a basic data on filters used for the multiband

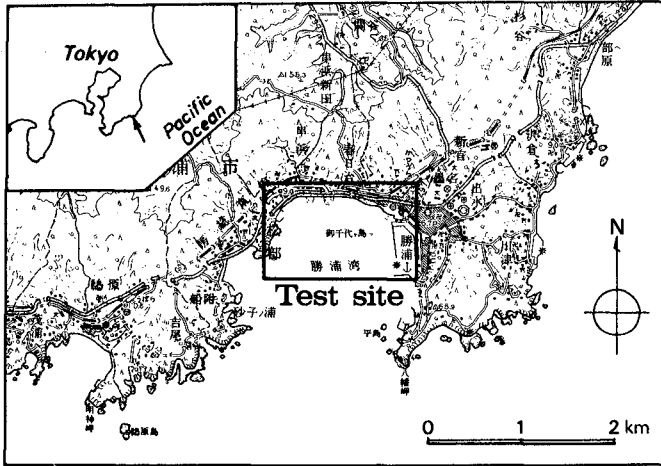


Figure 1 Test site.

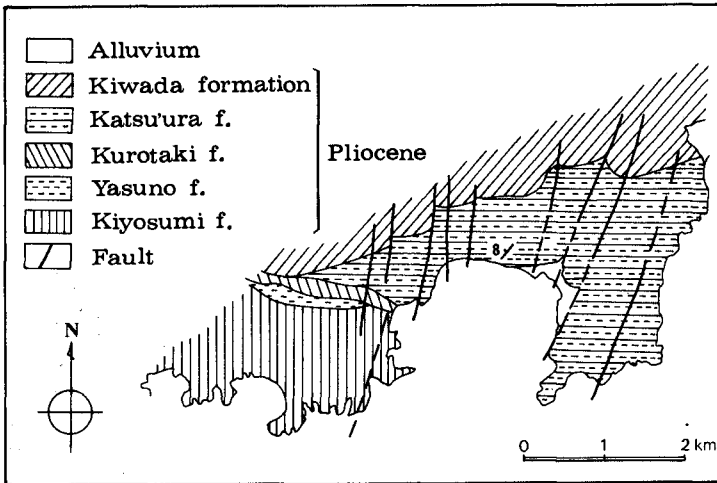


Figure 2 Geology around the test site.

photography with the aim of sounding a shallow-water area.

The process imagery through the image enhancement or processing devices has been widely used to extract various information from photographs ( American Society of Photogrammetry, 1975, pp. 611-813 ). However, these devices are expensive. The imagery processed from conventional color photographs by applying only filters without using any expensive equipment is also considered to be useful. But, the availability of this low-cost process imagery has not yet been tested with the exact sea or ground truths. The second purpose of the present study is to examine this availability from the view point of the data acquisition for coastal processes studies.

### TEST SITE

The test site is a shallow-water area at the head of the Katsu'ura Bay located on the Pacific coast of Japan ( Fig. 1 ). The bay is a semicircular shape bordered by coastal cliffs made of Pliocene sedimentary rocks ( Fig. 2 ). The alternation of sandstone and siltstone strata of Katsu'ura formation ( strike: N40-50E, dip: 5-10N ) forms the cliff at the test site. A narrow bay-head beach develops with an alongshore distance of 1.3 km. The direction of wave approach is nearly normal to the beach. Approximate tidal range at spring tide is 1.5 m, while at neap tide is 0.7 m.

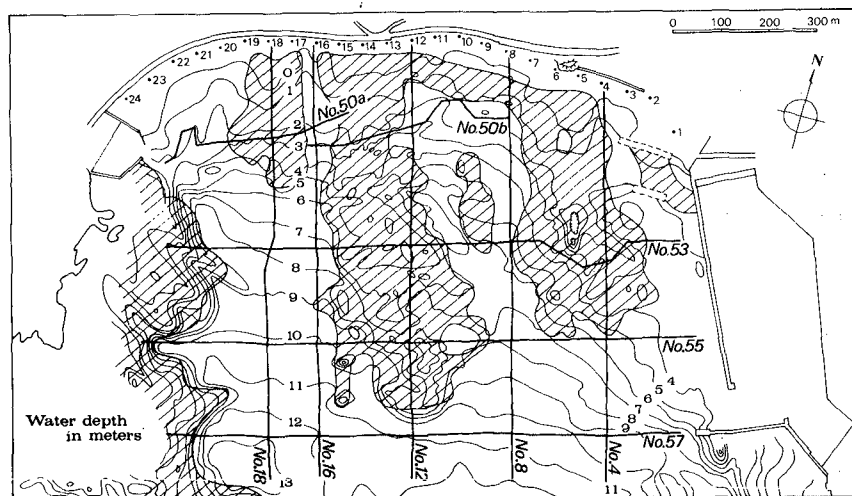


Figure 3 Submarine topography and the area of exposed bedrock ( hatched area ).

Underwater topographical and geological characteristics of the test site are that (1) the seabed consists of portions made of medium sand and of exposed bedrock ( Katsu'ura formation ) ( Fig. 3 ), and (2) the bedrock region is located higher than the adjacent sand bottom, forming an abrasion platform ( Fig. 4 ). The higher bedrock-region induces the convergence of wave energy ( Sunamura and Horikawa, 1976 ); the energy convergence produces breaking waves even in a calm sea.

The main reasons for the selection of this area as the test site are that (1) water is clear, and (2) both the bedrock and the sandy areas have no regional color variations, respectively.

#### AERIAL PHOTOGRAPHY

The flight plan was made paying much attention to the exclusion of the sun's glitter on aerial photographs. Along the flight lines ( Fig. 5 ), the test site was photographed by using a Cessna aircraft at an altitude of about 1,000 m during three days from November 27 to 29, 1974, under different wave conditions. Approximately 60 per cent overlap along the flight lines and 30 per cent side lap were obtained.

A synchronized camera system consisting of four Hasselblad cameras was employed. One of them was used for color photographs, and the remaining three cameras were used for multiband photographs, i.e., 3-band black-and-white photographs applying Kodak Wratten filters 29, 58, and 90, respectively ( Fig. 6 ). Films for the color and the multiband photographs were Kodak Aerocolor Negative 2445 and Kodak Tri-X Aerographic 2403, respectively. Table 1 shows the film/filter/camera combinations and additional photographic data.

#### GROUND AND SEA TRUTH MEASUREMENTS

Prior to photographing, two kinds of work were made for the water depth determination test: (1) a bathymetric survey and (2) submarine installation of white targets. The former was done along 32 ranges 25 m apart, set up perpendicularly to the shoreline; the inshore region including the backshore and foreshore was measured by using a transit, staff, and tape, while the offshore region up to a water depth of several meters was surveyed with the aid of an echo sounder. The latter was done by using five squares with a length of 1.8 m each ( Fig. 7 ), which were placed at a water depth of 1 to 5 m with a vertical interval of 1 m ( Fig. 8 ). The location of the target installation is shown in Fig. 9.

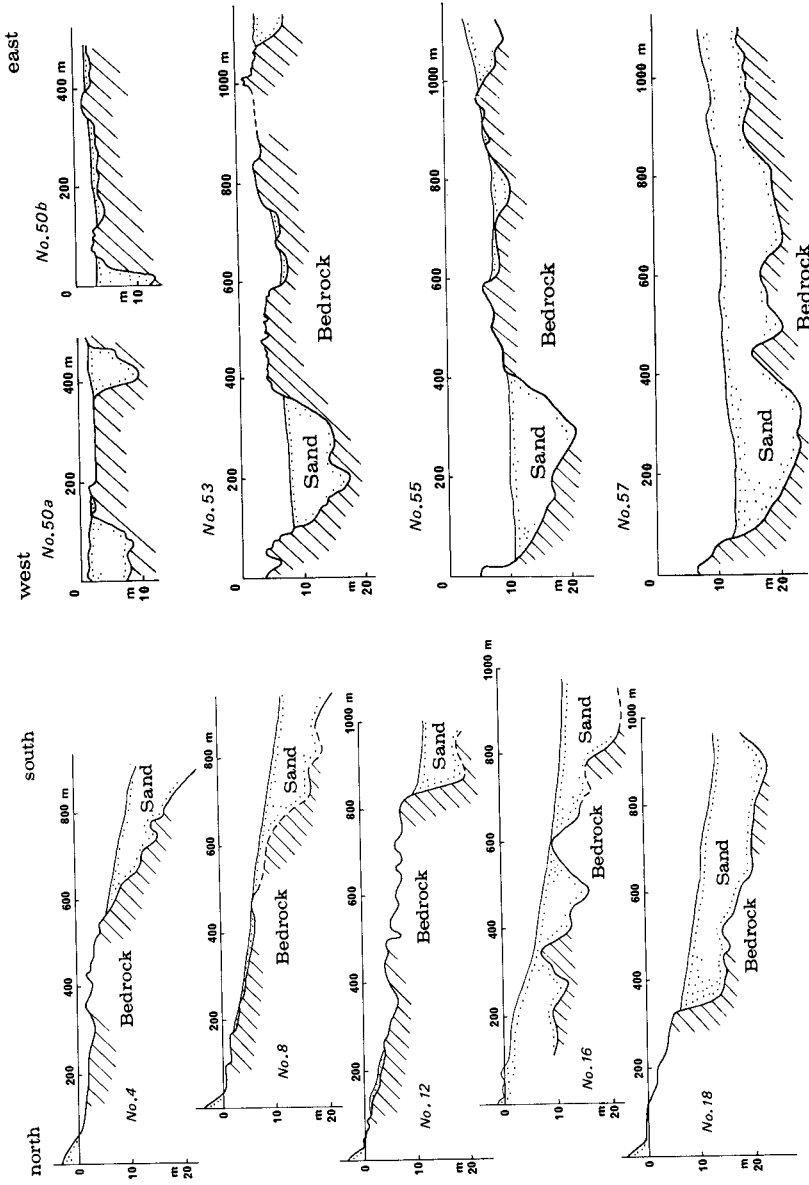


Figure 4 Geological cross-sections along survey lines shown in Fig. 3.

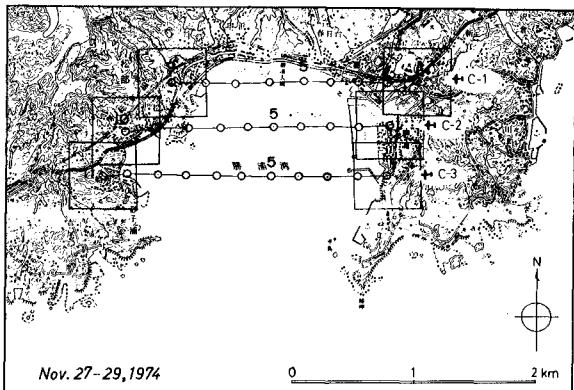


Figure 5  
Flight lines.

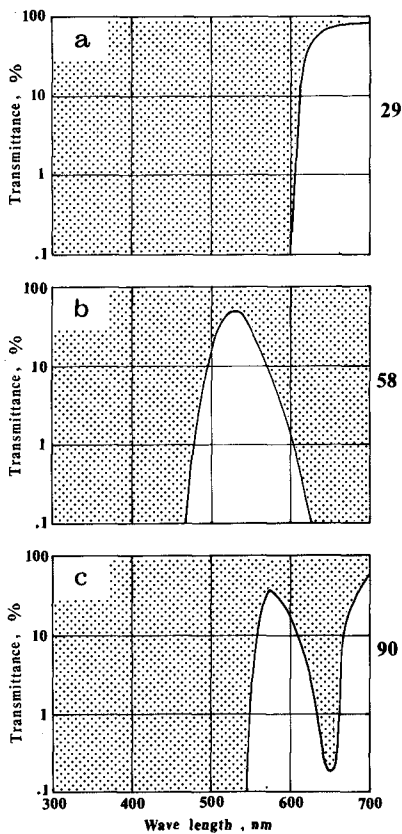


Figure 6  
Filters used for the multiband  
photography.

Table 1 Film/filter/camera combinations.

Film*	Filter**	Camera***	Lens† & focal length	f	Shutter speed	Remarks
2403	58	MK 70	100.94 mm	5.6	1/250	Multiband photo
2403	90	500EL	100	4	1/250	
2403	29	500EL	100	5.6	1/500	
2445	2B	500EL	100	8	1/500	Color photo

\* Kodak

\*\* Kodak Wratten

\*\*\* Hasselblad

† Zeiss

Figure 7  
Sketch showing a submerged target.

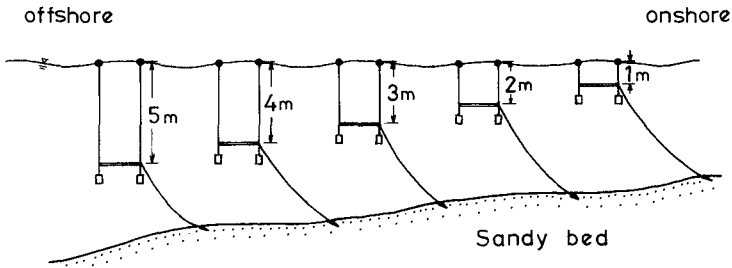
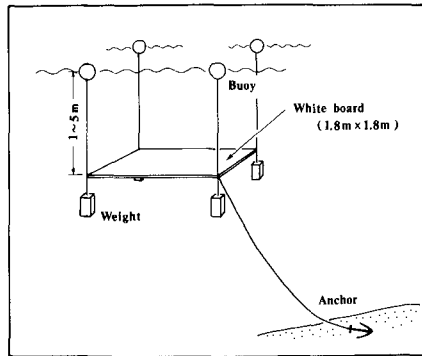


Figure 8 Schematic diagram showing underwater installation of targets.

Table 2 Wave and tidal conditions at the time of photography.

Time and date	Waves		Tide level
	Breaker height	Period	
	$H_b$	$T$	
12:00-13:00 Nov. 27, 1974	ab. 1 m	9-10 sec	0.4-0.5 m above MSL
12:00-13:00 Nov. 28, 1974	ab. 2	10-11	0.4-0.5 above MSL
12:00-13:00 Nov. 29, 1974	ab. 1.5	ab. 10	0.35-0.45 above MSL

The wave condition during the aerial photography is summarized in Table 2. The test site is characterized by the existence of an alongshore variation in the height of breaking waves: higher breakers are observed in the bedrock region compared to the adjacent sand area. The "breaker height" in Table 2 denotes a time-averaged value in the bedrock region.

#### DATA ANALYSES AND RESULTS

##### (1) Filter Test for Water Depth Determination

Two methods have been developed concerning the quantitative photographic bathymetry ( American Society of Photogrammetry, 1975, pp. 1574-1584 ): (1) photogrammetric method using stereoscopic ( three-dimensional ) measuring techniques, and (2) transparency method using photographic-density measuring techniques. The present study applied the latter method for the availability check of the filters used in the multiband photography. Photographs with no influence of suspended material are needed for the quantification of the photographic density-water depth relation. The photographs of November 27 were used here, because the degree of sediment suspension was the lowest due to the calmest sea during the three-day investigation ( see Table 2 ). The photographic density was measured by applying a micro-densitometer ( Rhesca Model PPA-250 ) on the positive transparencies. The density output was expressed in terms of volts.

Figure 10 shows a linear relationship between water depth and the photo-density on the submerged targets; this relation was obtained from the photographs with a Wratten 90 filter. Results from the Wratten 29- and 58-filtered photographs presented the similar relation to Fig. 10, although a considerable scatter of the data

points was seen.

Two measuring lines, C-16 and C-30 ( see Fig. 9 ), were sorted out from the 32 survey ranges for the photo-density measurement over the natural submarine bottom: C-16 traverses the bedrock area, while C-30 the sandy area. Both lines have little influence of sediment suspension. The correlation between the density and water depth becomes worse in order of the Wratten 90-, 58-, and 28-filtered photographs. Figure 11 is the best result, obtained from the Wratten 90-filtered photographs, showing some scatter of the data points. The lack of data points in the bedrock region shallower than a water depth of 1.5 m is due to the presence of surf zone. The result of the natural seabed shows the exponential relation ( Fig. 11 ), while the target test presents the linear one ( Fig. 10 ). The reason for this difference is unknown.

The light transmission characteristics of coastal water show that maximum transmittance occurs with the 500-600 nm ( green ) range of electromagnetic spectrum ( Duntley, 1963; Lockwood et al., 1974 ). Therefore, one can expect that a Wratten 58 filter having a bandwidth of 460-620 nm ( see Fig. 6(b) ) could be optimum for the bathymetric use. However, the present study indicates that a Wratten 90 filter was the best. The possible reason for this is as follows:

In the visible-region electromagnetic spectrum, the shorter wavelength radiation is more sensitive to the scattering by fine particles suspended in the atmosphere and the ocean than the longer wavelength radiation. A Wratten 58 filter transmits wavelengths of 460-500 nm ( a part of blue region ), allowing the record of the atmospheric and oceanic scattering; this masks the underwater information recorded by the green-region electromagnetic waves. Therefore a perfectly blue-cut filter like a Wratten 90 filter would produce the best result.

## (2) Availability Check of Low-Cost Process Imagery

Three kinds of images were processed in a laboratory from the color photographs by utilizing blue ( Kodak Wratten filter 94 ), green ( 93 ) and red ( 92 ) filters, respectively ( see Fig. 12 ). In this processing, was used a separation film whose sensitivity covered a wavelength range of 400-700 nm. The imagery, printed on the separation film at first, was finally printed out on the ordinary printing paper. This was black-and-white negative imagery. Figure 13 shows one example of the process imagery.

Figure 13(a) shows a low-contrast image, produced by the atmos-

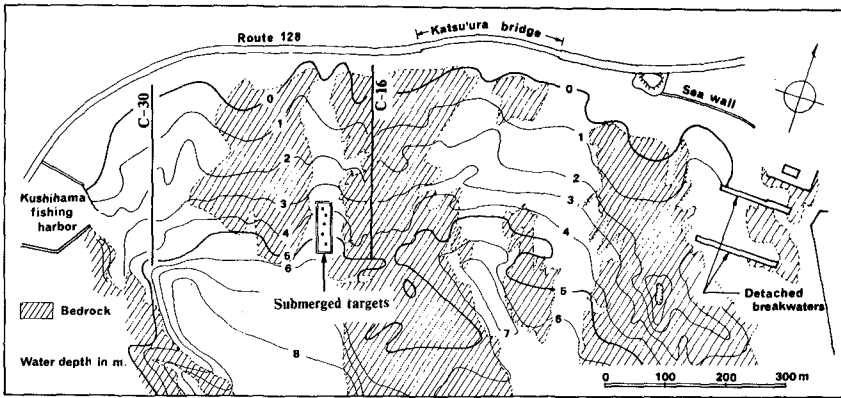


Figure 9 Locations of the submerged targets and the survey lines ( C-16 and 30 ), used for water depth determination test.

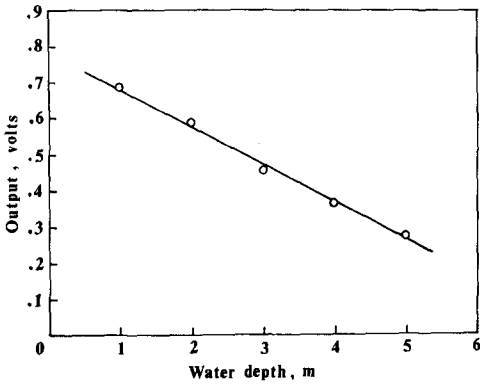


Figure 10 Water depth vs. photographic density on the submerged targets.

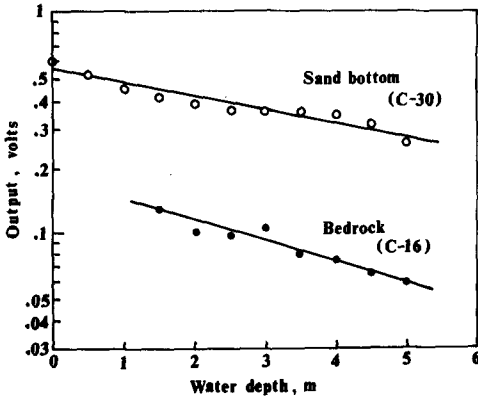


Figure 11 Water depth vs. photographic density on the natural seabed.

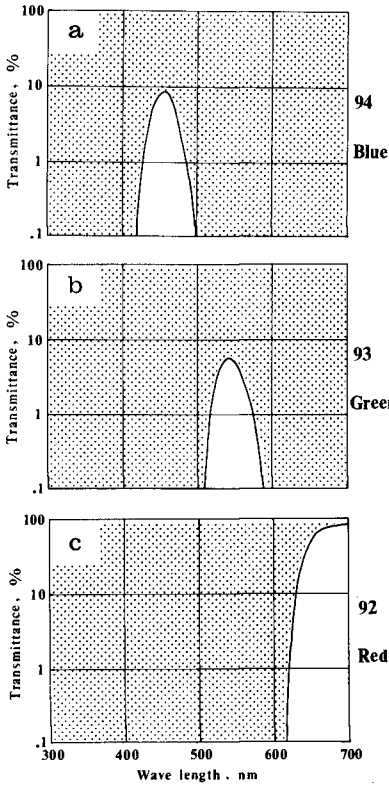


Figure 12  
 Filters used for image processing  
 from the color photographs.

pheric and oceanic scattering of the 400 to 500 nm-length waves. This indicates that blue-filtered photographs are not available for use in the interpretation of a shallow-water environment.

Figure 13(b) allows the visualization of submarine bedrock features, because the green filter transmits wavelengths of 510 to 580 nm, which have the capability of recording underwater details to maximum depth. Since wave breaking and sediment suspension deteriorate the underwater information, the photographs taken under the calmest sea condition should be used for the submarine investigation. The green-filtered images of November 27 were applied for the delineation of the linear features on the exposed bedrock; the result is shown in Fig. 14.

Figure 13(c) exhibits a clear image of rip current pattern, i.e., flow pattern of water discolored by suspended material. In



(a) Blue-filtered



(b) Green-filtered



(c) Red-filtered

Figure 13 Process imagery from the color photograph taken on November 28, 1974, by using blue, green, and red filters.

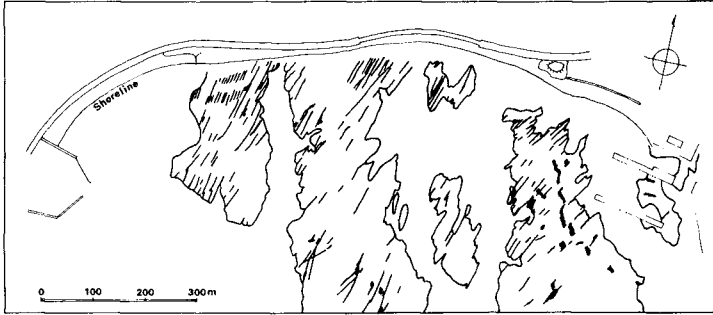


Figure 14 Linear features on exposed submarine bedrock, depicted from the green-filtered imagery of November 27, 1974.

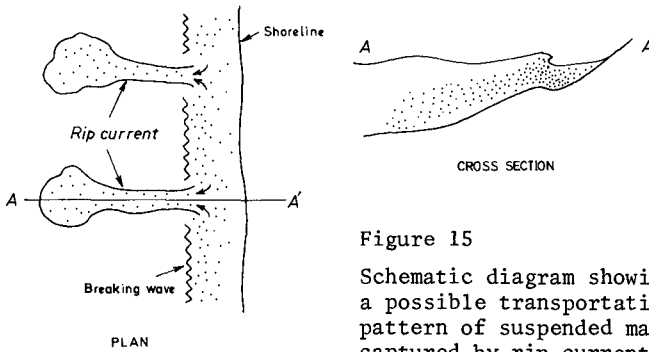


Figure 15 Schematic diagram showing a possible transportation pattern of suspended matter captured by rip currents.

the red region of electromagnetic spectrum, the degree of water penetration is inferior as compared to the green-region wavelengths. This means that the red-filtered imagery supplies shallower-water information than the green-filtered imagery does. The material transported offshore by rip currents would probably be suspended to a certain height over the seabed ( Fig. 15 ). Therefore the red-filtered imagery is preferable for tracing the pattern of sediment-laden rip currents. Figure 16 shows the rip current patterns depicted from the red-filtered images of the three-day data; the solid lines indicate certainty and the dashed lines show uncertainty as to the delineation of the flow pattern. The degree of rip current development increases with increasing breaker height.

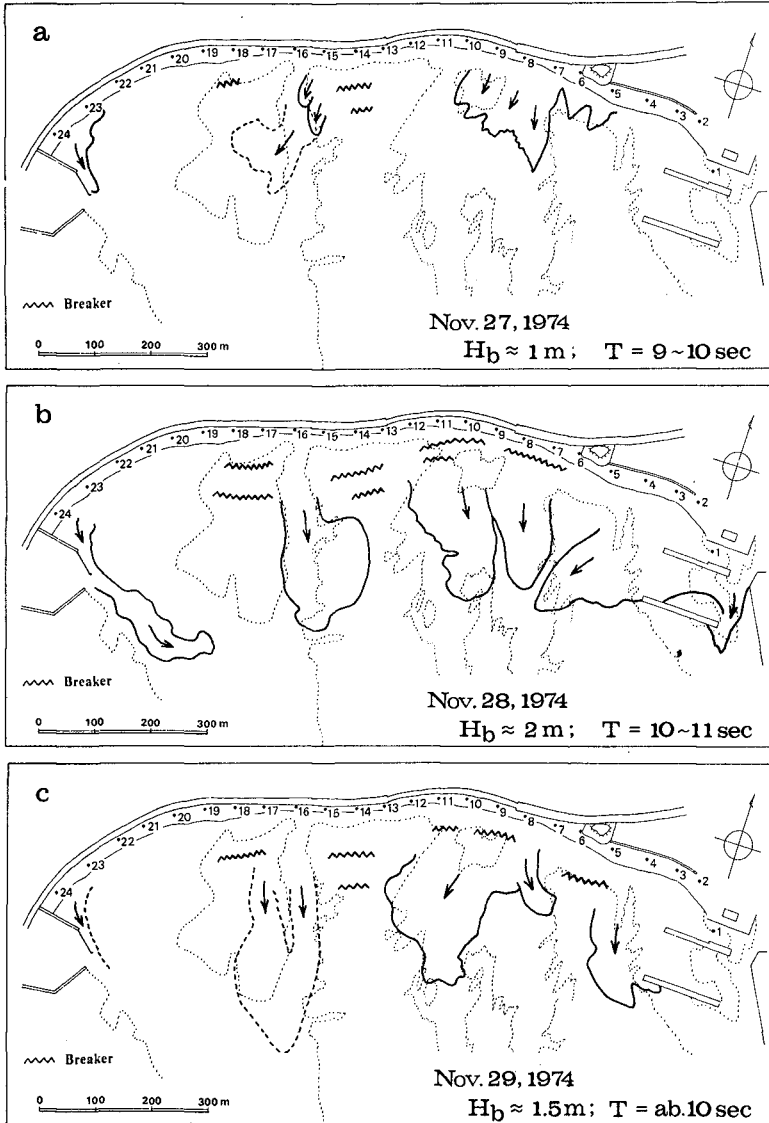


Figure 16 Rip current patterns depicted from the red-filtered imagery.

## CONCLUSIONS

A perfectly blue-cut filter is useful for the multiband photography having the purpose of shallow-water bathymetry by the transparency method. However, there is a limitation that the photographs should be taken under calm sea conditions, because suspended material and surf zone make it difficult to read accurately the photographic density.

The low-cost process imagery from conventional color photographs by using pertinent filters is available for use in the study of coastal processes.

## ACKNOWLEDGMENTS

This study was financially supported by National Institute of Resources, Science and Technology Agency, Japan. Helpful information of photographic engineering given by Dr. Y. Shima of Chiba University is greatly appreciated.

## REFERENCES

- American Society of Photogrammetry, 1975, Manual of Remote Sensing. R. G. Reeves, Editor-in-chief, American Society of Photogrammetry, Falls Church, Virginia, 2144 pp.
- Duntley, S. Q., 1963, Light in the sea. Jour. Optical Soc. Am., vol. 53, pp. 214-233.
- Lockwood, H. E., Perry, L., Sauer, G. E., and Lamar, N. T., 1974, Water depth penetration film test. Photogrammetric Eng., vol. 40, pp. 1303-1314.
- Magoon, O. T. and Pirie, D. M., 1972, Remote sensing in the study of coastal processes. Proc. 13th Coastal Eng. Conf., Vancouver, pp. 2027-2043.
- Pestrong, R., 1969, Multiband photos for a tidal marsh. Photogrammetric Eng., vol. 35, pp. 453-470.
- Stafford, D. B., 1972, Coastal engineering applications of aerial remote sensing. Proc. 13th Coastal Eng. Conf., Vancouver, pp. 2045-2064.
- Sunamura, T. and Horikawa, K., 1976, Field investigation of sediment transport pattern in a closed system. Proc. 15th Coastal Eng. Conf., Honolulu, pp. 1240-1257.